Geophysical Research Letters

RESEARCH LETTER
10.1029/2024GL112776

Gulf Stream Near Cape Hatteras Modulates Sea Level Variability Along the Southeastern Coast of North America

Tianning Wu[1] **and Ruoying He**[1]

[1]North Carolina State University, Raleigh, NC, USA

Abstract Studies suggest a strong link between low-frequency sea level variability in the South Atlantic Bight (SAB) and open ocean dynamics. However, the mechanisms driving this connection remain unclear. By analyzing a high-resolution, three-dimensional baroclinic ocean reanalysis, we identify a pathway that links open ocean dynamics to SAB coastal sea level variability through the shelf edge near Cape Hatteras. Gulf Stream meanders in this region induce sea level fluctuations that propagate along the entire SAB shelf. Using an idealized barotropic model, we further demonstrate that topographic waves mediate the propagation of the Gulf Stream signal onto the shelf. Moreover, the Gulf Stream variability is driven by zonal wind stress in the Northwest Atlantic, which is likely modulated by the North Atlantic Oscillation. These findings offer new insights into regional sea level prediction and contribute to broader climate research efforts.

Plain Language Summary This study examines how open ocean changes influence sea level along the South Atlantic Bight (SAB). While previous research highlighted a link between sea level changes and open ocean dynamics, the exact process was unclear. Using high-resolution model data, we identified how Gulf Stream shifts near Cape Hatteras affect SAB sea levels, driven by winds over the Northwest Atlantic and likely tied to the North Atlantic Oscillation. These findings enhance our understanding of SAB coastal sea level and offer insight for predicting coastal sea level change and studying the climate.

Key Points:

- Gulf Stream meanders near Cape Hatteras cause significant sea level fluctuations at the nearby shelf edge
- Shelf-edge sea level anomalies near Cape Hatteras propagate into the South Atlantic Bight via topographic waves
- Gulf Stream variability near Cape Hatteras connects open ocean dynamics to sea level in the South Atlantic Bight

Supporting Information:

Supporting Information may be found in the online version of this article.

Correspondence to:

R. He,
rhe@ncsu.edu

Citation:

Wu, T., & He, R. (2025). Gulf Stream near Cape Hatteras modulates sea level variability along the southeastern coast of North America. *Geophysical Research Letters*, *52*, e2024GL112776. https://doi.org/10.1029/2024GL112776

Received 27 SEP 2024
Accepted 19 FEB 2025

Author Contributions:

Conceptualization: Tianning Wu, Ruoying He
Data curation: Ruoying He
Formal analysis: Tianning Wu
Funding acquisition: Ruoying He
Investigation: Tianning Wu, Ruoying He
Methodology: Tianning Wu, Ruoying He
Project administration: Ruoying He
Resources: Ruoying He
Software: Tianning Wu, Ruoying He
Supervision: Ruoying He
Validation: Tianning Wu
Visualization: Tianning Wu
Writing – original draft: Tianning Wu
Writing – review & editing: Ruoying He

1. Introduction

Sea level along the North American East Coast (NAEC) has risen faster than the global average in recent decades (Dangendorf et al., 2023; O'Donnell et al., 2024; Piecuch et al., 2018; Sallenger et al., 2012; Sweet & Park, 2014), with severe environmental and socioeconomic impacts on coastal communities (Ohenhen et al., 2024; O'Donnell et al., 2024). Moreover, sea level fluctuations over timescales from months to decades often exceed mean sea level rise at NAEC and intensify coastal flooding (Ezer & Atkinson, 2014; Yin, 2023). Understanding regional sea level drivers is crucial for sea level prediction and building coastal resilience.

Sea level fluctuations along the NAEC have shown complex spatial and temporal patterns (Diabaté et al., 2021; Little et al., 2021). Since the 1990s, the South Atlantic Bight (SAB) and the Mid-Atlantic Bight (MAB), separated by the Cape Hatteras, North Carolina, have experienced different rates of sea level rise. MAB saw faster sea level rise before 2010 (Sallenger et al., 2012; Yin & Goddard, 2013), while SAB has outpaced MAB since then (Domingues et al., 2018; Valle-Levinson et al., 2017). This discrepancy has been attributed to the difference in forcing mechanisms (e.g., Wang et al., 2024), including different coastal response to Gulf Stream variability (Ezer, 2019).

SAB sea level variability is largely attributed to open ocean dynamics in the Subtropical Gyre (Dangendorf et al., 2023; Domingues et al., 2018; Hong et al., 2000; Volkov et al., 2019, 2023; Wang et al., 2024; Yin & Goddard, 2013). Within the Subtropical Gyre, the Gulf Stream is located over the continental slope of SAB and generally follows the topography (Figure 1a). Due to Gulf Stream's large cross-stream sea level gradients and proximity to the shelf, its transport variations induce geostrophic ocean topography anomalies that influence coastal sea level (Ezer, 2019). The Gulf Stream carries signals from large-scale variability, such as the North Atlantic Oscillation (NAO) and the Atlantic Meridional Overturning Circulation (Caesar et al., 2018; Joyce et al., 2000; McCarthy et al., 2018; Piecuch & Beal, 2023), thus plays an important role in inducing open ocean variability to the coast. Previous studies primarily focused on the relationship between SAB sea level and Gulf Stream strength, and anti-correlations were found between them over timescales from days to decades (Chi et al., 2023; Ezer, 2017; Park & Sweet, 2015; Woodworth et al., 2017). However, it remains unclear how changes

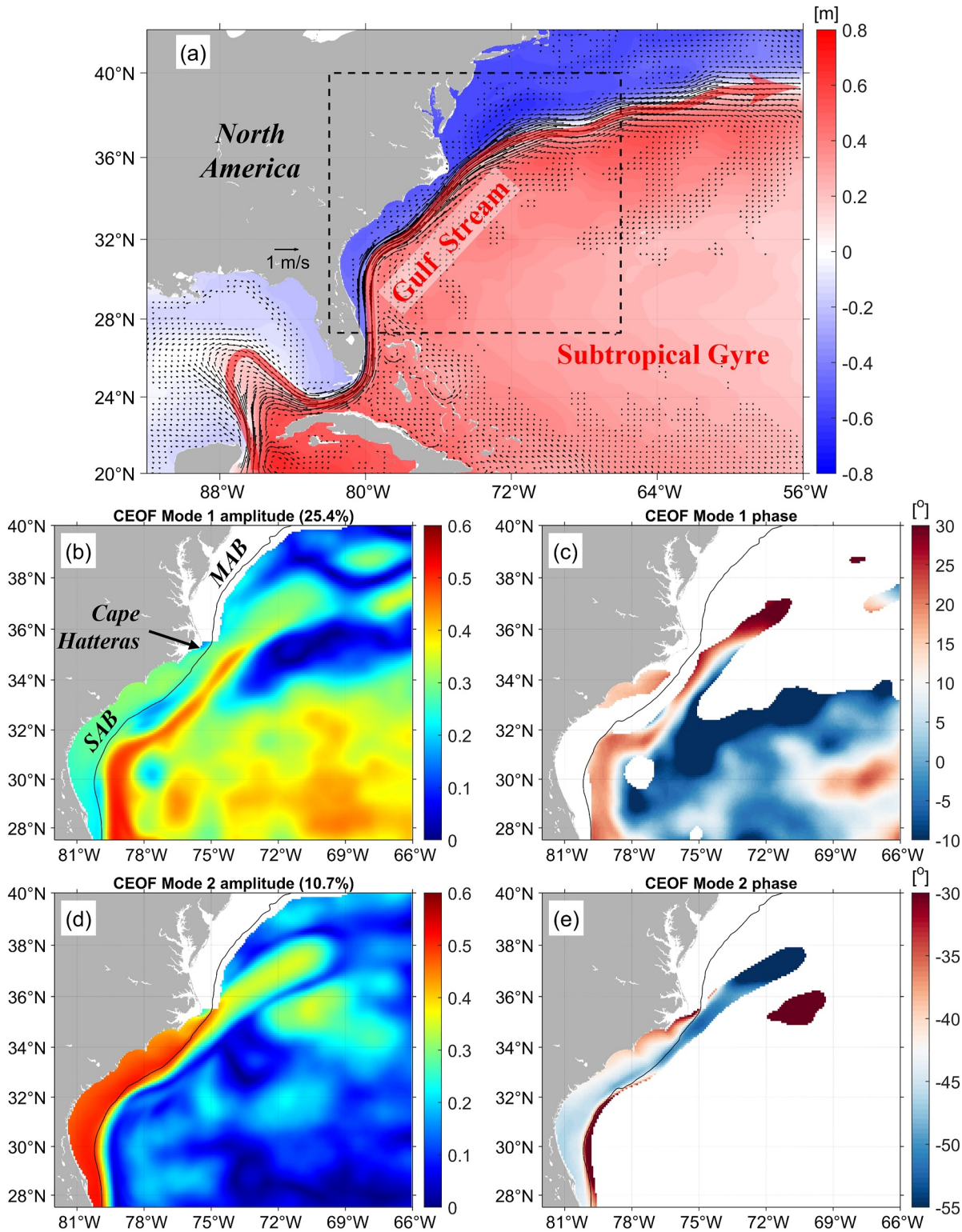

Figure 1. Regional ocean circulation and CEOF analysis on SLA. (a) Mean SSH (color shading) and surface current (vectors, showing only where speed >0.05 m/s) of the 30-year ocean reanalysis. The red arrow illustrates the Gulf Stream mean path. The dashed region represents the CEOF analyzed area shown in (b–e). (b) Spatial amplitude map of the first mode. (c) Spatial phase map of the first mode, showing only areas where the amplitude in (b) is higher than 0.3 for clarity. (d) Same as (b) but for the second mode. (e) Spatial phase map of the second mode, showing only areas where the amplitude in (d) exceeds 0.3 for clarity. The black contour marks the 200-m isobath.

in the Gulf Stream position affect SAB coastal sea level, particularly as the Gulf Stream becomes less stable after encountering the Charleston Bump (Bane & Dewar, 1988; Zeng & He, 2016).

This study investigated the connection between Gulf Stream variability near Cape Hatteras and low-frequency (seasonal-to-decadal timescale) sea level fluctuations in SAB using high-resolution ocean reanalysis. Then, an idealized barotropic model was utilized to investigate the mechanism driving this relationship. This research further examined how large-scale climate variability in the North Atlantic drives Gulf Stream variability near Cape Hatteras, establishing a pathway that links open ocean variability to SAB sea level change.

2. Data and Methods

2.1. Ocean Reanalysis

A 30-year data-assimilative, high-resolution, and well-validated ocean reanalysis was developed to capture daily ocean dynamics in the Northwest Atlantic from 1993 to 2022. Using the Regional Ocean Modeling System (Shchepetkin & McWilliams, 2005) with Ensemble Kalman Filter data assimilation system (Sakov & Sandery, 2017), the reanalysis encompasses the northwestern Atlantic Ocean (Figure S1 in Supporting Information S1), operating on a 1/25th degree (approximately 4 km) grid with 50 terrain-following vertical levels, refined near the surface and bottom to better resolve boundary layer dynamics. The model's meteorological forcing, including wind, atmospheric pressure, and surface heat and freshwater fluxes, was obtained from European Center for Medium-Range Weather Forecasts Reanalysis v5 (ERA5). It assimilates various in-situ and remote sensing observations, including sea surface height (SSH), sea surface temperature (SST), and temperature/salinity (T/S) profiles to ensure accurate representation of the ocean state. This configuration effectively captures boundary currents and mesoscale features, particularly around Cape Hatteras, where shelf and deep ocean interactions occur at a narrow continental margin (Seim et al., 2022). In this study, the 3-month rolling average of SSH and velocity fields were used to filter out short-term variations and focus on low-frequency sea level changes linked to open ocean variabilities. The sea level anomaly (SLA) was derived by removing the linear trend and seasonal cycle in the SSH.

2.2. Complex Empirical Orthogonal Function (CEOF) Analysis

While standard Empirical Orthogonal Function (EOF) analysis identifies stationary oscillations, Complex EOF (CEOF) analysis can be applied to identify propagating signals. CEOF has been widely used in oceanography and atmospheric science (Hannachi et al., 2007; Navarra & Simoncini, 2010), including in sea level research (Volkov et al., 2022; Wise et al., 2020). CEOF analyzes a Hilbert transform to the scalar input, which enables the detection of propagating signals. For a scalar input field $\mathbf{D}(\mathbf{x},t)$, where $\mathbf{x}$ is grid point index, and t is time index, the complex field is:

$$\widehat{\mathbf{D}}(\mathbf{x},t) = \mathbf{D}(\mathbf{x},t) + i\mathcal{H}(\mathbf{D}(\mathbf{x},t)) \tag{1}$$

where $\mathcal{H}()$ is the Hilbert transform and i is the imaginary unit. The real part is the original scalar input field, while the Fourier components of the imaginary part have the same amplitudes as those of the real part but with a phase shift of $\pi/2$ in time.

The CEOFs and Complex Principal Components (CPCs) of $\widehat{\mathbf{D}}$ are obtained through Singular Value Decomposition:

$$\widehat{\mathbf{D}}(\boldsymbol{x},t) = \sum_k \mathbf{u}_k(\mathbf{x})\sigma_k\mathbf{v}_k(t) \tag{2}$$

where $\mathbf{u}_k(\mathbf{x})$ is the kth mode of CEOF and $\sigma_k\mathbf{v}_k(t)$ is its CPC.

The spatial amplitude function $\mathbf{a}_k(\mathbf{x})$ and spatial phase function $\boldsymbol{\theta}_k(\mathbf{x})$ are:

$$\mathbf{a}_k(\mathbf{x}) = \mathbf{u}_k(\mathbf{x}) \cdot \mathbf{u}_k^*(\mathbf{x}) \tag{3}$$

$$\boldsymbol{\theta}_k(\mathbf{x}) = \text{atan}[Im(\mathbf{u}_k(\mathbf{x}))/Re(\mathbf{u}_k(\mathbf{x}))] \tag{4}$$

where $Im()$ and $Re()$ represent the real and imaginary parts, respectively.

The temporal amplitude function $\mathbf{b}_k(t)$ and temporal phase function $\boldsymbol{\phi}_k(t)$ are:

$$\mathbf{b}_k(t) = \sigma_k \mathbf{v}_k(t) \cdot \sigma_k \mathbf{v}_k^*(t) \tag{5}$$

$$\boldsymbol{\phi}_k(t) = \text{atan}\left[Im\left(\sigma_k \mathbf{v}_k(t)\right)/Re\left(\sigma_k \mathbf{v}_k(t)\right)\right] \tag{6}$$

Spatial and temporal amplitude functions show how energetic each mode is in space and time. The spatial phase function provides wavelength and direction, while the temporal phase function shows the time evolution of signal propagation. Spatial amplitude was normalized by the standard deviation of respective temporal amplitude for inter-mode comparisons.

We applied CEOF analysis to the SLA fields along the U.S. east coast ocean to investigate the propagation of sea level signals (Figure 1). According to previous studies, sea level variability in SAB mainly comes from two drivers: coastally trapped signals propagating from north of Cape Hatteras and offshore signals originating from the interior Subtropical Gyre (e.g., Wise et al., 2020). To focus on the offshore signals, we masked the SLA over MAB shelf in the CEOF analysis, excluding the coastally trapped signals.

2.3. Idealized Model for Arrested Topographic Wave in SAB

When offshore sub-inertial sea level anomalies impose onto the continental slope, they tend to propagate along f/H contours (f: Coriolis parameter; H: water depth) in order to conserve potential vorticity (PV). As a result, anomalies are deflected along the slope as topographic waves in the direction of Kelvin wave (i.e., equatorward along NAEC). This process insulates the shelf from open ocean anomalies and is commonly referred to as PV barrier.

Csanady (1978) suggested that bottom friction allows offshore anomalies to penetrate the PV barrier with attenuated magnitudes, forming what are known as arrested topographic waves (ATWs). The extent and scale of onshore penetration depend on the shelf bathymetry and the influence of bottom friction (Huthnance, 2004; Wise et al., 2020; Wu, 2021).

To explore the mechanism by which Gulf Stream-induced offshore sea level anomalies penetrate the PV barrier on the SAB slope and shelf break, we used an idealized barotropic model based on the ATW theory. This model helps us understand how Gulf Stream variability near Cape Hatteras impacts the entire SAB. It is based on a set of steady-state, linearized 2-D barotropic momentum equations with linear bottom friction (Wu, 2021):

$$-fv = -g\frac{\partial \eta}{\partial x} - \frac{ru}{h}, \tag{7}$$

$$fu = -g\frac{\partial \eta}{\partial y} - \frac{rv}{h}, \tag{8}$$

$$\frac{\partial (uh)}{\partial x} + \frac{\partial (vh)}{\partial y} = 0 \tag{9}$$

where $u(x, y, t)$ and $v(x, y, t)$ are horizontal velocity components in x- and y-direction, f is the Coriolis parameter on the β-plane, g is gravity acceleration, $h(x, y)$ is water depth, $\eta(x, y, t)$ is dynamic SSH, and r is bottom friction coefficient.

The domain of the idealized model covers the SAB shelf and upper slope (depth <500 m), with the grid and bathymetry subset from the ocean reanalysis grid (Figure S1 in Supporting Information S1). Gradient boundary conditions were applied at open boundaries, and a first-order upstream scheme was employed to numerically solve the governing equations. Initial velocity and SSH were set to zero. To simulate the Gulf Stream-induced SSH variability near Cape Hatteras, a constant SSH value of $\eta = 1$ m was imposed at the shelf edge (33.5°N to 35°N, 200–500 m isobaths), and there is no wind forcing. The bottom friction coefficient ($r = 5 \times 10^{-4}$ m/s) was adopted from Csanady (1978). Since we focus on seasonal-to-decadal time scale, a steady-state model is adequate to simulate the response of SAB sea level to low frequency open-ocean variability.

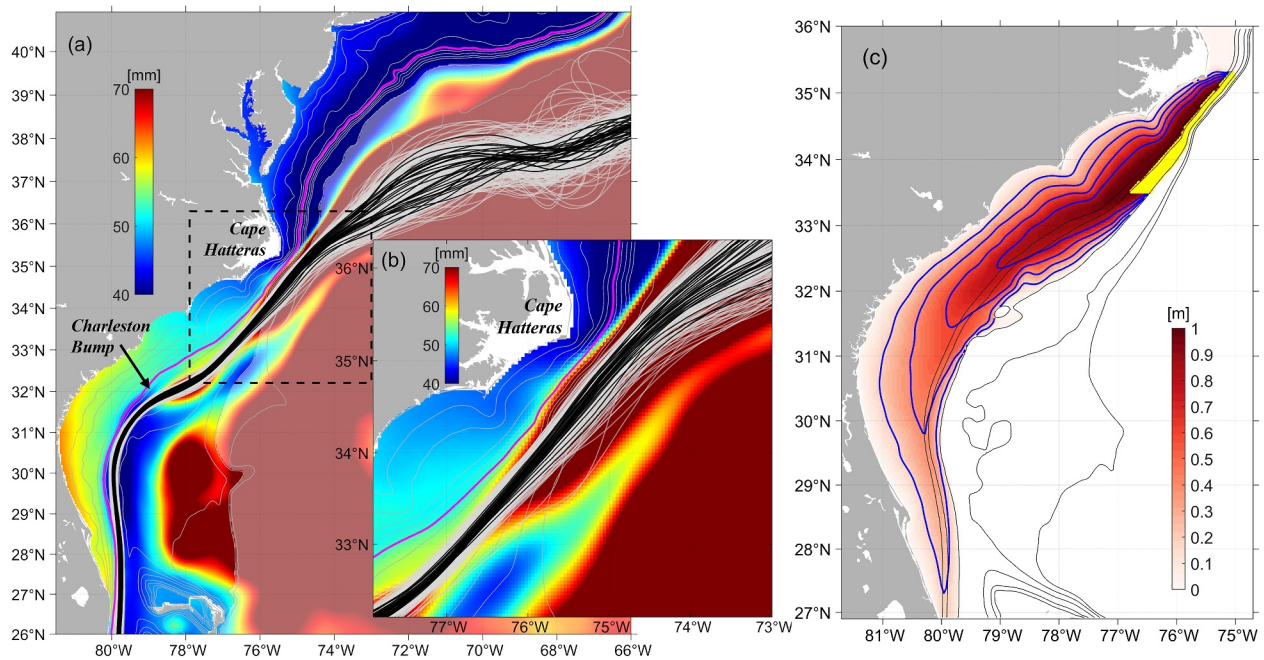

Figure 2. Sea level variability and Gulf Stream path in the ocean reanalysis, and the SSH output from the idealized model simulation. (a) Color shading represents the standard deviation map of SLA from 1993 to 2022. Areas with depth greater than 2,000 m are grayed out for clarity. Off-white lines represent the Gulf Stream path, defined by the 0.5-m contours in the 3-month rolling averaged SSH. Black lines represent the Gulf Stream path defined by the 0.5 m contours in annual mean SSH. (b) An enlarged view of the dashed region in (a), highlighting the area around Cape Hatteras. Gray contours represent isobaths, with the 200-m isobath highlighted in magenta. (c) Idealized model output. Color shading represents SSH in meters. Blue contours marks 0.2-, 0.4-, 0.6-, and 0.8-m SSH. The yellow shaded area is the forcing area of $\eta = 1$ m. Gray contours represent isobaths.

3. Results

3.1. Propagation of SLA Signals

The first two CEOF modes reveal dominant patterns of sea level signal propagation (Figures 1b–1e). In the first mode, the spatial amplitude map exhibits an offshore pattern mainly in the interior Subtropical Gyre and the offshore flank of the Gulf Stream, with weak amplitude over the SAB shelf, indicating limited coastal influence (Figure 1b). The spatial phase map indicates a westward propagation from the interior to the Gulf Stream, likely associated with the long Rossby wave propagation in the deep ocean (Figure 1c).

The second mode's spatial amplitude map reveals an onshore pattern centered on the SAB shelf, following the Gulf Stream downstream of Cape Hatteras (Figure 1d), suggesting substantial impact on SAB sea level. The spatial phase map indicates southwestward propagation along the Gulf Stream onto the shelf, with the signal landing at the shelf edge (33.5°N–35°N) before moving onshore (Figure 1e). Wise et al. (2020) also observed this penetration of sea level signals from the shelf edge into SAB in their CEOF analysis of idealized models, and Ezer (2016) suggested that variations in the Gulf Stream transport can generate coastal trapped waves in the SAB. This mode suggests that Gulf Stream variability near Cape Hatteras is a key driver of SAB sea level variability, with a fast propagation speed. The phase difference between Gulf Stream near Cape Hatteras and Southern SAB is about 15° (Figure 1e), and the temporal phase takes about a month to evolve 15° (i.e., 360° in 2 years; Figure S2 in Supporting Information S1), hence the signal travels from the Gulf Stream near Cape Hatteras to southern SAB in about a month.

3.2. The Hotspot of Sea Level Variability at Shelf Edge

The second mode of CEOF analysis suggests that the sea level variability on the shelf edge near Cape Hatteras is a key driver of SAB sea level change. To further investigate this, we examined the standard deviation map of SLA (Figures 2a and 2b). Over seasonal and longer timescales, sea level variability in the coastal ocean is smaller than

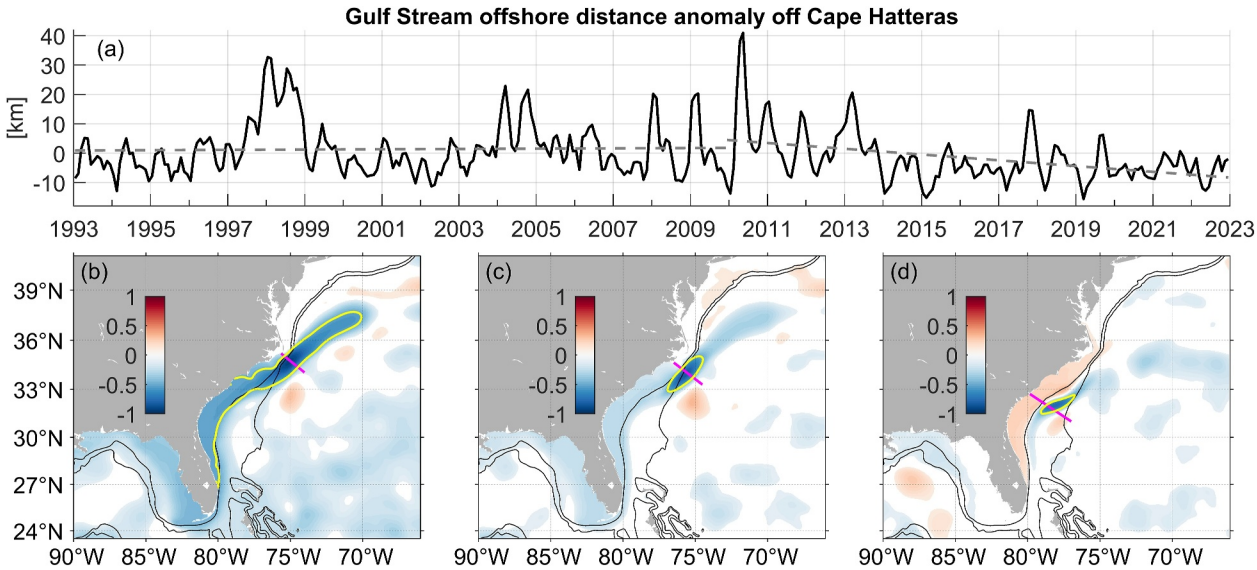

Figure 3. Correlation between Gulf Stream variability and SLA (a) Gulf Stream offshore distance anomaly near Cape Hatteras calculated from the magenta transect shown in (b). Trends before and after 2010 are shown in dashed gray line. (b) Correlation coefficient between Gulf Stream offshore distance anomaly at the magenta transect and SLA at each grid point. Insignificant values ($p \geq 0.05$) are not shown. The yellow contour represents the −0.5 correlation coefficient. Gray contours represent 200-m and 1000-m isobath. (c, d) are same as (b) but for different transects marked as the magenta line in respective panels.

in the open ocean, with stronger variability in SAB compared to MAB. Along the shelf edge, variability is generally low except between 33.5°N and 35°N near Cape Hatteras.

The hotspot of sea level variations is likely linked to Gulf Stream variability. The Gulf Stream follows the upper continental slope along the SAB before separating near Cape Hatteras (Figure 2a). In SAB, it closely follows slope topography until deflecting seaward at the Charlston Bump, where it becomes less stable (Bane & Dewar, 1988; Zeng & He, 2016). Further downstream, Gulf Stream variability increases near Cape Hatteras, generating large sea level fluctuations at the shelf edge (Figure 2b). Onshore Gulf Stream shifts result in positive SLA at the shelf edge, and vice versa.

3.3. Response of SAB Sea Level to Offshore Variability Near Cape Hatteras

The shift in Gulf Stream path generates large sea level variability at the upper slope and shelf edge near Cape Hatteras (Figures 2a and 2b). However, it is unclear whether this offshore variability is able to cross the PV barrier and reach the SAB coastal ocean. To investigate the underlying mechanism and assess the influence of the Gulf Stream-induced sea level variability on the SAB shelf, we conducted an idealized simulation based on the ATW theory (see Section 2.3).

The idealized simulation shows that sea level anomalies at the shelf edge near Cape Hatteras are able to influence the entire SAB, with a larger impact on the outer shelf compared to the coast (Figure 2c). Nonetheless, the coastal impact ranges from 10% to 20% of the imposed anomaly at the shelf edge. This supports the hypothesis that Gulf Stream variability near Cape Hatteras modulates SAB sea level. Note that this model does not include boundary Kelvin wave. In reality, the coastal sea level at each latitude should reflect a combination of ATW from the shelf edge and boundary Kelvin wave from higher latitudes (Minobe et al., 2017).

3.4. Relating Sea Level Change in SAB With Gulf Stream Variability

To test the relationship between Gulf Stream variability near Cape Hatteras and SAB sea level, we calculated the correlation coefficient between SLA and Gulf Stream offshore distance at three SAB transects from 1993 to 2022 (Figure 3). The Gulf Stream offshore distance was derived from the 3-month rolling averaged velocity fields from the ocean reanalysis. At each timeframe, the Gulf Stream core was defined as the location of maximum surface speed, and its offshore distance was measured as the distance from the core to the 200-m isobath at each transect. The offshore distance anomaly was obtained by removing the season cycle from such time series (Figure 3a).

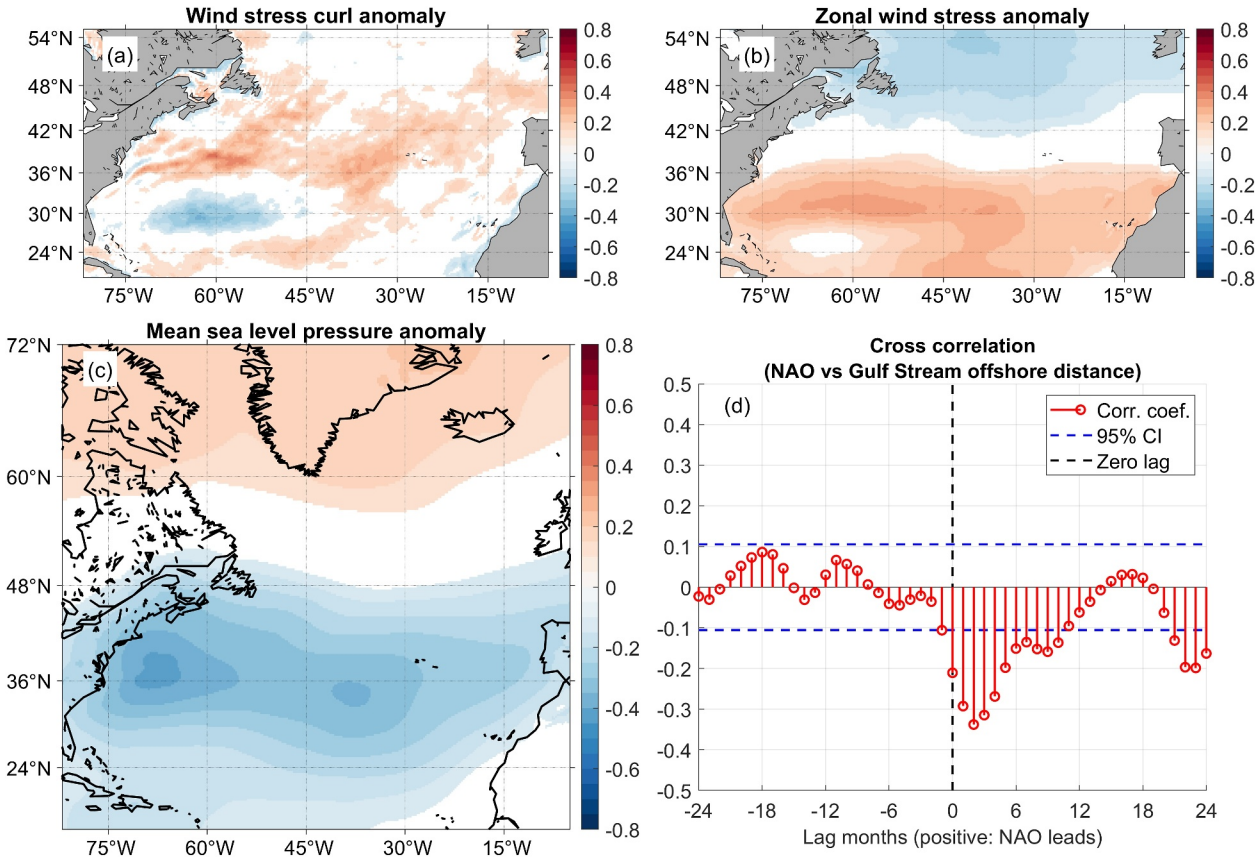

Figure 4. Gulf Stream variability near Cape Hatteras and climate variability in North Atlantic. (a) Lagged correlation coefficient map between Gulf Stream offshore distance near Cape Hatteras (Figure 3a) and wind stress curl anomaly, with wind stress curl anomaly leading the Gulf Stream by 3 months. Both variables are 3-month rolling averaged. Insignificant values ($p \geq 0.05$) are not shown. (b) Same as (a) but for zonal wind stress anomaly. (c) Same as (a) but for mean sea level pressure anomaly. (d) Cross-correlation coefficients between Gulf Stream offshore distance near Cape Hatteras and NAO. Blue dashed lines indicate the 95% confidence level. The black dashed line denotes zero lag. Wind stress curl anomaly, zonal wind stress anomaly, and mean sea level pressure anomaly are derived from monthly mean fields from ERA5 by removing their respective seasonal cycles. The NAO index is the monthly principal component-based Hurrell NAO index.

The Gulf Stream offshore distance anomaly near Cape Hatteras strongly correlates with SAB SLA (Figure 3b). High correlation is observed on the SAB shelf and extends northeast along the Gulf Stream past Cape Hatteras. The correlation even extends into the Gulf of Mexico. Such pattern aligns with the CEOF analysis (Figure 1e) and the idealized model (Figure 2c). The negative correlation indicates that negative SLA in SAB corresponds to the offshore movement of the Gulf Stream near Cape Hatteras, and vice versa. Further south, the correlation weakens due to lower Gulf Stream variability and/or increased distance between the Gulf Stream and the shelf edge (Figures 3c and 3d). Notably, there was a decreasing trend in Gulf Stream offshore distance near Cape Hatteras after 2010, which contributed to the accelerated sea level rise in SAB (Figure 3a). This multidecadal variation in the Gulf Stream is likely associated with basin-scale wind-driven variability in the North Atlantic, which have been proposed as a driver of the rapid SAB sea level rise since 2010 (Dangendorf et al., 2023).

3.5. Connection With Large-Scale Climate Variability

Studies have shown that the Gulf Stream position downstream of Cape Hatteras is influenced by large-scale atmospheric forcings, such as wind stress curl and zonal wind stress (Gangopadhyay et al., 1992; Gifford et al., 2024; Seidov et al., 2019; Silver et al., 2021). The Gulf Stream path in its extension region (i.e., after separation from the Cape Hatteras) was observed to covary with zero wind stress curl line (Seidov et al., 2019) and maximum wind stress curl line (Gifford et al., 2024). The lagged-correlation map indicates that wind stress curl anomalies over the extension region lead the Gulf Stream's onshore-offshore movements near Cape Hatters by 3 months (Figure 4a). This relationship is mainly caused by zonal wind stress anomalies south of the Gulf Stream extension (Figure 4b), which can be explained by the Parsons-Veronis model for the separation of western

boundary currents (Gangopadhyay et al., 1992; Parsons, 1969; Veronis, 1973). For example, an eastward zonal wind stress anomaly at the Gulf Stream separation latitude induces a southward transport anomaly in the upper ocean due to Ekman drift. It drives the shoaling of thermocline, causing its outcrop near the western boundary to shift further offshore. Because the Gulf Stream is located at the thermocline outcrop line, this process drives the Gulf Stream to move offshore.

The correlation map between mean sea level pressure anomaly and the Gulf Stream offshore distance shows a dipole pattern similar to the NAO pressure loading (Figure 4c). Cross-correlations between the NAO index and Gulf Stream offshore distance reveal that the Gulf Stream movement lags NAO by 3 months, suggesting that NAO-induced zonal wind stress anomaly may influence the position of Gulf Stream. However, the relatively low correlation coefficient (0.35) indicates that NAO only partially explains the Gulf Stream variability. Notably, the subtropical pressure pattern in Figure 4c is centered over the Northwest Atlantic, differing from typical NAO pressure loading. It suggests that the position and shape of the Azores High may also have substantial influences on the Gulf Stream variability. Nevertheless, Gulf Stream variability near Cape Hatteras serves as a critical connection between the large-scale open ocean dynamics and coastal sea level change in SAB.

4. Conclusions

Earlier studies suggested that open ocean dynamics contribute to low-frequency sea level variability in SAB. However, the mechanism allowing these anomalies to cross the PV barrier at the continental margin and affect SAB coastal sea level is an open question. Using a long-term high-resolution ocean reanalysis and an idealized barotropic model, we identified a pathway connecting open ocean dynamics to SAB coastal sea level through the shelf edge near Cape Hatteras. Gulf Stream variability in the region causes substantial sea level fluctuations at the shelf edge, which propagate equatorward along the SAB shelf and penetrate onshore due to bottom friction. This explains the strong correlations between Gulf Stream offshore distance near Cape Hatteras and SAB SLA.

The Gulf Stream's position near Cape Hatteras is linked to large-scale atmospheric dynamics, as shown by its correlations with wind stress curl and zonal wind stress anomalies. These correlations align with the Parsons-Veronis hypothesis, which explains Gulf Stream shifts through zonal wind stress anomalies at its separation latitude. NAO likely influences Gulf Stream variability near Cape Hatteras by modulating the zonal wind stress.

Gulf Stream variability near Cape Hatteras plays an important role in connecting SAB coastal sea level to large-scale open ocean dynamics. Since sea level anomalies induced at the shelf edge near Cape Hatteras only propagate southward into SAB, it contributes to sea level difference across Cape Hatteras. It explains the relationship between such sea level difference and Gulf Stream latitudinal movement west of 69°W described by Diabaté et al. (2021). Moreover, the Gulf Stream has moved closer to the shelf edge near Cape Hatteras, which contributed to the accelerated sea level rise in SAB since 2010. Findings of our study provide practical insights for sea level prediction, flood risk assessments, and coastal resilience on the U.S. southeast coast. Additionally, historical tide gauge records along the NAEC could help infer past Gulf Stream variability, offering valuable data for climate research.

Data Availability Statement

The Northwest Atlantic ocean reanalysis is available at https://thredds.secoora.org/thredds/catalog/secoora-cnaps-30-year/catalog.html. Monthly ERA5 data were retrieved from https://cds.climate.copernicus.eu/datasets/reanalysis-era5-single-levels-monthly-means (Hersbach et al., 2023). The monthly Hurrell NAO index was retrieved from https://climatedataguide.ucar.edu/climate-data/hurrell-north-atlantic-oscillation-nao-index-pc-based (Hurrell et al., 2024).

Acknowledgments
Research support provided through NSF Grants OCE-1559178 and OCE-1851421, RISE-2019758, OCE-2206052, CNS-2223844, NOAA Grant NA16NOS0120028 is much appreciated. We thank Drs. Harvey Seim, Sarah Larson, Ke Chen, and Joseph Zambon for many insightful discussions throughout this study.

References

Bane, J. M., & Dewar, W. K. (1988). Gulf Stream bimodality and variability downstream of the Charleston bump. *Journal of Geophysical Research*, *93*(C6), 6695–6710. https://doi.org/10.1029/jc093ic06p06695

Caesar, L., Rahmstorf, S., Robinson, A., Feulner, G., & Saba, V. (2018). Observed fingerprint of a weakening Atlantic Ocean overturning circulation. *Nature*, *556*(7700), 191–196. https://doi.org/10.1038/s41586-018-0006-5

Chi, L., Wolfe, C. L. P., & Hameed, S. (2023). Reconsidering the relationship between gulf stream transport and dynamic sea level at U.S. East Coast. *Geophysical Research Letters*, *50*(9), e2022GL102018. https://doi.org/10.1029/2022gl102018

Csanady, G. T. (1978). The arrested topographic wave. *Journal of Physical Oceanography*, *8*(1), 47–62. https://doi.org/10.1175/1520-0485(1978)008<0047:tatw>2.0.co;2

Dangendorf, S., Hendricks, N., Sun, Q., Klinck, J., Ezer, T., Frederikse, T., et al. (2023). Acceleration of U.S. Southeast and Gulf coast sea-level rise amplified by internal climate variability. *Nature Communications*, *14*(1), 1935. https://doi.org/10.1038/s41467-023-37649-9

Diabaté, S. T., Swingedouw, D., Hirschi, J. J.-M., Duchez, A., Leadbitter, P. J., Haigh, I. D., & McCarthy, G. D. (2021). Western boundary circulation and coastal sea-level variability in Northern Hemisphere oceans. *Ocean Science*, *17*(5), 1449–1471. https://doi.org/10.5194/os-17-1449-2021

Domingues, R., Goni, G., Baringer, M., & Volkov, D. (2018). What caused the accelerated sea level changes along the U.S. East Coast during 2010–2015? *Geophysical Research Letters*, *45*(24), 13367–13376. https://doi.org/10.1029/2018gl081183

Ezer, T. (2016). Can the Gulf Stream induce coherent short-term fluctuations in sea level along the US East Coast? A modeling study. *Ocean Dynamics*, *66*(2), 207–220. https://doi.org/10.1007/s10236-016-0928-0

Ezer, T. (2017). A modeling study of the role that bottom topography plays in Gulf Stream dynamics and in influencing the tilt of mean sea level along the US East Coast. *Ocean Dynamics*, *67*(5), 651–664. https://doi.org/10.1007/s10236-017-1052-5

Ezer, T. (2019). Regional differences in sea level rise between the mid-Atlantic bight and the South Atlantic bight: Is the Gulf Stream to blame? *Earth's Future*, *7*(7), 771–783. https://doi.org/10.1029/2019ef001174

Ezer, T., & Atkinson, L. P. (2014). Accelerated flooding along the U.S. East Coast: On the impact of sea-level rise, tides, storms, the Gulf Stream, and the North Atlantic Oscillations. *Earth's Future*, *2*(8), 362–382. https://doi.org/10.1002/2014ef000252

Gangopadhyay, A., Cornillon, P., & Watts, D. R. (1992). A test of the Parsons–Veronis hypothesis on the separation of the Gulf Stream. *Journal of Physical Oceanography*, *22*(11), 1286–1301. https://doi.org/10.1175/1520-0485(1992)022<1286:atotph>2.0.co;2

Gifford, I., Gangopadhyay, A., Andres, M., Oliver, H., Gawarkiewicz, G., & Silver, A. (2024). Synchronicity of the Gulf Stream path downstream of Cape Hatteras and the region of maximum wind stress curl. *Scientific Reports*, *14*(1), 18479. https://doi.org/10.1038/s41598-024-68461-0

Hannachi, A., Jolliffe, I. T., & Stephenson, D. B. (2007). Empirical orthogonal functions and related techniques in atmospheric science: A review. *International Journal of Climatology*, *27*(9), 1119–1152. https://doi.org/10.1002/joc.1499

Hersbach, H., Bell, B., Berrisford, P., Biavati, G., Horányi, A., Sabater, J. M., et al. (2023). ERA5 monthly averaged data on single levels from 1940 to present. *Copernicus Climate Change Service (C3S) Climate Data Store (CDS)*. https://doi.org/10.24381/cds.f17050d7

Hong, B. G., Sturges, W., & Clarke, A. J. (2000). Sea level on the U.S. East Coast: Decadal variability caused by Open Ocean wind-curl forcing. *Journal of Physical Oceanography*, *30*(8), 2088–2098. https://doi.org/10.1175/1520-0485(2000)030<2088:slotus>2.0.co;2

Hurrell, J., & Phillips, A., & NCAR. (2024). The climate data guide: Hurrell North Atlantic Oscillation (NAO) index (PC-based). Retrieved from https://climatedataguide.ucar.edu/climate-data/hurrell-north-atlantic-oscillation-nao-index-pc-based

Huthnance, J. M. (2004). Ocean-to-shelf signal transmission: A parameter study. *Journal of Geophysical Research*, *109*(C12), C12029. https://doi.org/10.1029/2004jc002358

Joyce, T. M., Deser, C., & Spall, M. A. (2000). The relation between decadal variability of subtropical mode water and the North Atlantic Oscillation*. *Journal of Climate*, *13*(14), 2550–2569. https://doi.org/10.1175/1520-0442(2000)013<2550:trbdvo>2.0.co;2

Little, C. M., Piecuch, C. G., & Ponte, R. M. (2021). North American East Coast sea level exhibits high power and spatiotemporal complexity on decadal timescales. *Geophysical Research Letters*, *48*(15), e2021GL093675. https://doi.org/10.1029/2021gl093675

McCarthy, G. D., Joyce, T. M., & Josey, S. A. (2018). Gulf stream variability in the context of quasi-decadal and multidecadal Atlantic climate variability. *Geophysical Research Letters*, *45*(20), 11257–11264. https://doi.org/10.1029/2018gl079336

Minobe, S., Terada, M., Qiu, B., & Schneider, N. (2017). Western boundary sea level: A theory, rule of thumb, and application to climate models. *Journal of Physical Oceanography*, *47*(5), 957–977. https://doi.org/10.1175/jpo-d-16-0144.1

Navarra, A., & Simoncini, V. (2010). A guide to empirical orthogonal functions for climate data analysis. https://doi.org/10.1007/978-90-481-3702-2

O'Donnell, K. L., Bernhardt, E. S., Yang, X., Emanuel, R. E., Ardón, M., Lerdau, M. T., et al. (2024). Saltwater intrusion and sea level rise threatens U.S. rural coastal landscapes and communities. *Anthropocene*, *45*, 100427. https://doi.org/10.1016/j.ancene.2024.100427

Ohenhen, L. O., Shirzaei, M., Ojha, C., Sherpa, S. F., & Nicholls, R. J. (2024). Disappearing cities on US coasts. *Nature*, *627*(8002), 108–115. https://doi.org/10.1038/s41586-024-07038-3

Park, J., & Sweet, W. (2015). Accelerated sea level rise and Florida Current transport. *Ocean Science*, *11*(4), 607–615. https://doi.org/10.5194/os-11-607-2015

Parsons, A. T. (1969). A two-layer model of Gulf Stream separation. *Journal of Fluid Mechanics*, *39*(3), 511–528. https://doi.org/10.1017/s0022112069002308

Piecuch, C. G., & Beal, L. M. (2023). Robust weakening of the Gulf Stream during the past four decades observed in the Florida straits. *Geophysical Research Letters*, *50*(18), e2023GL105170. https://doi.org/10.1029/2023gl105170

Piecuch, C. G., Huybers, P., Hay, C. C., Kemp, A. C., Little, C. M., Mitrovica, J. X., et al. (2018). Origin of spatial variation in US East Coast sea-level trends during 1900–2017. *Nature*, *564*(7736), 400–404. https://doi.org/10.1038/s41586-018-0787-6

Sakov, P., & Sandery, P. (2017). An adaptive quality control procedure for data assimilation. *Tellus A: Dynamic Meteorology and Oceanography*, *69*(1), 1318031. https://doi.org/10.1080/16000870.2017.1318031

Sallenger, A. H., Doran, K. S., & Howd, P. A. (2012). Hotspot of accelerated sea-level rise on the Atlantic coast of North America. *Nature Climate Change*, *2*(12), 884–888. https://doi.org/10.1038/nclimate1597

Seidov, D., Mishonov, A., Reagan, J., & Parsons, R. (2019). Resilience of the Gulf Stream path on decadal and longer timescales. *Scientific Reports*, *9*(1), 11549. https://doi.org/10.1038/s41598-019-48011-9

Seim, H. E., Savidge, D., Andres, M., Bane, J., Edwards, C., Gawarkiewicz, G., et al. (2022). Overview of the processes driving exchange at cape Hatteras program. *Oceanography*. https://doi.org/10.5670/oceanog.2022.205

Shchepetkin, A. F., & McWilliams, J. C. (2005). The regional oceanic modeling system (ROMS): A split-explicit, free-surface, topography-following-coordinate oceanic model. *Ocean Modelling*, *9*(4), 347–404. https://doi.org/10.1016/j.ocemod.2004.08.002

Silver, A., Gangopadhyay, A., Gawarkiewicz, G., Taylor, A., & Sanchez-Franks, A. (2021). Forecasting the Gulf Stream path using buoyancy and wind forcing over the North Atlantic. *Journal of Geophysical Research: Oceans*, *126*(8), e2021JC017614. https://doi.org/10.1029/2021jc017614

Sweet, W. V., & Park, J. (2014). From the extreme to the mean: Acceleration and tipping points of coastal inundation from sea level rise. *Earth's Future*, *2*(12), 579–600. https://doi.org/10.1002/2014ef000272

Valle-Levinson, A., Dutton, A., & Martin, J. B. (2017). Spatial and temporal variability of sea level rise hot spots over the eastern United States. *Geophysical Research Letters*, *44*(15), 7876–7882. https://doi.org/10.1002/2017gl073926

Veronis. (1973). Model of world ocean circulation_ I. Wind-driven two-layer. *Journal of Marine Research*, *31*(3). Retrieved from https://elischolar.library.yale.edu/journal_of_marine_research/1270

Volkov, D. L., Lee, S., Domingues, R., Zhang, H., & Goes, M. (2019). Interannual sea level variability along the southeastern seaboard of the United States in relation to the gyre-scale heat divergence in the North Atlantic. *Geophysical Research Letters*, *46*(13), 7481–7490. https://doi.org/10.1029/2019gl083596

Volkov, D. L., Schmid, C., Chomiak, L., Germineaud, C., Dong, S., & Goes, M. (2022). *Interannual to decadal sea level variability in the subpolar North Atlantic: The role of propagating signals* (Vol. 2022, pp. 1–39). EGUsphere. https://doi.org/10.5194/egusphere-2022-354

Volkov, D. L., Zhang, K., Johns, W. E., Willis, J. K., Hobbs, W., Goes, M., et al. (2023). Atlantic meridional overturning circulation increases flood risk along the United States southeast coast. *Nature Communications*, *14*(1), 5095. https://doi.org/10.1038/s41467-023-40848-z

Wang, O., Lee, T., Frederikse, T., Ponte, R. M., Fenty, I., Fukumori, I., & Hamlington, B. D. (2024). What forcing mechanisms affect the interannual sea level co-variability between the northeast and southeast coasts of the United States? *Journal of Geophysical Research: Oceans*, *129*(1), e2023JC019873. https://doi.org/10.1029/2023jc019873

Wise, A., Polton, J. A., Hughes, C. W., & Huthnance, J. M. (2020). Idealised modelling of offshore-forced sea level hot spots and boundary waves along the North American East Coast. *Ocean Modelling*, *155*, 101706. https://doi.org/10.1016/j.ocemod.2020.101706

Woodworth, P. L., Maqueda, M. Á. M., Gehrels, W. R., Roussenov, V. M., Williams, R. G., & Hughes, C. W. (2017). Variations in the difference between mean sea level measured either side of Cape Hatteras and their relation to the North Atlantic Oscillation. *Climate Dynamics*, *49*(7–8), 2451–2469. https://doi.org/10.1007/s00382-016-3464-1

Wu, H. (2021). Beta-plane arrested topographic wave as a linkage of Open Ocean forcing and mean shelf circulation. *Journal of Physical Oceanography*, *51*(3), 879–893. https://doi.org/10.1175/jpo-d-20-0195.1

Yin, J. (2023). Rapid decadal acceleration of sea level rise along the U.S. East and Gulf Coasts during 2010-2022 and its impact on hurricane-induced storm surge. *Journal of Climate*, 1–38. https://doi.org/10.1175/jcli-d-22-0670.1

Yin, J., & Goddard, P. B. (2013). Oceanic control of sea level rise patterns along the East Coast of the United States. *Geophysical Research Letters*, *40*(20), 5514–5520. https://doi.org/10.1002/2013gl057992

Zeng, X., & He, R. (2016). Gulf Stream variability and a triggering mechanism of its large meander in the South Atlantic bight. *Journal of Geophysical Research: Oceans*, *121*(11), 8021–8038. https://doi.org/10.1002/2016jc012077